Journal of Applied Electrochemistry **32**: 621–627, 2002.

Effect of thiourea and saccharin on the roughness of electrodeposited ultrathin nickel and cobalt layers

R.F. RENNER and K.C. LIDDELL*
Department of Chemical Engineering, Washington State University, Pullman, WA 99164-2710, USA
*(*author for correspondence)*

Received 29 August 2001; accepted in revised form 16 April 2002

Key words: cobalt, nickel, saccharin, surface roughness, thiourea

Abstract

Ni and Co films were produced by electrodeposition from plating baths containing either thiourea or saccharin. The effect of the organic additives on surface roughness was studied for the Ni-thiourea, Ni-saccharin, Co-thiourea and Co-saccharin systems. Layer thicknesses were varied from 1 to 10 nm and the additive concentration was varied from about 1 μM to 1 mM. Contact mode atomic force microscopy was used to measure both the root mean square (RMS) peak height (nm) and the areal peak density (μm^{-2}) of each film. Although the RMS peak height and areal density were both influenced by film thickness and by additive concentration, the two roughness measures provide complementary information on the layer morphology and growth mechanisms. The four systems studied responded differently to changes in the concentration of the added organic. For example, for films 8 nm thick, addition of 1.22×10^{-3} thiourea reduced the Ni peak density about 80%; in contrast, the Co peak density was increased over 180% by addition of 1.25×10^{-3} thiourea. Use of peak height and peak density data to infer growth mechanisms for ultrathin films is discussed.

1. Introduction

Organic additives are often used in electroplating operations to moderate deposit growth rates and control film quality. It is often assumed that additives act by preferentially adsorbing onto asperities on the cathode surface, thereby blocking the attachment of metal ions at those sites and favouring growth at other locations. However, detailed nucleation and growth mechanisms must be inferred from indirect evidence. Systematic studies of the influence of organic additives on deposit surface morphology are few, especially for the ultrathin layers that are important in microelectronics and data storage applications. Most of the available information applies to relatively thick layers (1–100 μm).

The purpose of this study was to measure the roughness of ultrathin nickel and cobalt layers as a function of both layer thickness (1–10 nm) and organic concentration (1 μM–1 mM). Deposit surfaces were examined by atomic force microscopy (AFM), and both RMS peak height and areal peak density were used to quantify the differences between samples as in our previous work on additive-free films [1]. The additives used were saccharin and thiourea, which are first and second class brighteners, respectively. First class brighteners reduce tensile stress in the deposit, an effect that should be dependent on deposit thickness. Second class brighteners have less predictable effects that depend on their concentration.

Radiotracer techniques have shown that both ^{35}S and ^{14}C are incorporated into Ni films plated from a thiourea-containing bath [2]. On a molar basis, the deposits contain much more sulfur than carbon, indicating that the organic decomposes [2, 3]. Incorporation of sulfur appears to be diffusion-controlled [4]. Progressive increases in the thiourea concentration lead to wide variations in the C:S ratio of the deposit [5].

Like thiourea, saccharin decomposes during Ni plating, and radiochemical experiments again indicated uptake of ^{35}S [6]. The proposed mechanism is controlled by both diffusion and Langmuir-type adsorption, and the density of adsorption sites appears to depend on plating conditions [3, 4]. Benzamide and *o*-toluenesulfonamide have been identified spectroscopically as the major decomposition products [7]; saccharin decomposes at roughly twice the rate sulfur is incorporated in the deposit.

The effects of saccharin on the texture of electrodeposited Ni are not clear. Saccharin has been reported by Nakamura et al. [8] and by Gao et al. [9] to cause the preferred orientation of an electrodeposited Ni lattice to shift to (111). However, these reports are inconsistent with those of Macheras et al. [10], who indicated that the [100] texture predominates for current densities less than

10 A dm^{-2}. The film thicknesses and current densities appear to be comparable in all three studies.

Atomic force microscopy has been used by Troyon and coworkers [11] to determine how saccharin affects the surface roughness of relatively thick Ni films. The RMS roughness of a 15 μm film was around 13 nm for galvanostatic plating with a current density of 400 A m^{-2}. Film roughness was somewhat dependent on plating conditions and decreased with an increase in the pH of the Watts-type electrolyte. Changes in roughness with deposit thickness were not addressed in this work.

Although there are several recent papers on the effects of additives in the plating of Co-containing alloys [12–15], similar work apparently has not been reported for pure Co deposits. Other recent work has employed more complex electrolytes than ours and has focused on Cu–Co multilayers [16] or on pulsed electrodeposition of Cu–Co alloys [17, 18]. As pointed out by Chassaing, variations in electrolyte composition appear to significantly affect current efficiency, and it is probable that deposition mechanisms are influenced as well.

2. Experimental details

Ni and Co layers were electrodeposited in a 170 mL Plexiglas cell. The films were plated on silicon substrates that had been precoated with a vapour deposited Cu layer which served as the cathode during deposition. The RMS peak height (defined below) of the copper-coated Si substrate was determined by AFM to be 0.7 ± 0.1 nm [19]. There was a 1.2 cm diameter hole in the cell for mounting the substrates; a metal plate was screwed on to prevent leakage. Indium wire was used to make contact between the Cu basal layer and a potentiostat. A Pt wire counter electrode and saturated calomel reference electrode (SCE) were used.

The plating bath compositions were similar to those of a Watts bath. The Ni solution contained 330 g dm^{-3} $NiSO_4 \cdot 6H_2O$ and 35 g dm^{-3} H_3BO_3; the pH was 3.2. The Co electrolyte was composed of 281 g dm^{-3} $CoSO_4 \cdot 6H_2O$ and 35 g dm^{-3} H_3BO_3; the pH was 3.4. Varying amounts of the organic additives, saccharin and thiourea were then added to the bath from freshly prepared stock solutions.

A computer-controlled potentiostat was used to apply the overpotential during deposition experiments. Both Co and Ni layers were plated from an unstirred solution at close to −1200 mV vs SCE. This potential was chosen following preliminary cyclic voltammetry experiments [19] in which large anodic peaks were observed when either of the additives of interest was added to either bath; −1200 mV was more negative than any such peak but also positive enough that visible hydrogen evolution was avoided. Although each experiment was carried out potentiostatically, the applied potential was adjusted slightly between experiments when an additive was present; this enabled a uniform steady state current density of approximately 0.5 mA cm^{-2} to be maintained, assuring that the rate of deposition was virtually the same for all samples. The maximum adjustment necessary was 50 mV. A series of samples was grown in separate experiments under identical conditions for each system (Ni-thiourea, Ni-saccharin, Co-thiourea, Co-saccharin) and each additive concentration chosen. Steady state currents were reached within 0.3 s. Given that the Ni and Co layers deposited are ~1 cm in diameter and typically 5–10 nm thick, the mass of each film is about 5 μg and could not be measured by the techniques available. Reported layer thicknesses in this work are nominal values calculated from the total cathodic charge passed as determined from the integrated current–time plots and without correcting for current efficiency; the nominal thickness was controlled by varying the deposition time.

An atomic force microscope (Digital Instruments) was used in contact mode to measure surface roughness using software provided by the manufacturer. Each sample was characterized by two methods: the root mean square (RMS) peak height, and the areal peak density. RMS peak height is a measure of vertical roughness and is defined by

$$H_{\mathrm{RMS}} = \left[\frac{1}{mn}\sum_{i=1}^{m}\sum_{j=1}^{n}\left(y_{ij}-\bar{y}\right)^2\right]^{1/2}$$

where m and n give the number of data points in the x and z directions, respectively; y_{ij} is the height of a data point and the mean elevation from the surface is given by

$$\bar{y} = \frac{1}{mn}\sum_{i=1}^{m}\sum_{j=1}^{n} y_{ij}$$

Areal peak density is calculated by measuring the number of peaks on the sample surface above a certain threshold height. To obtain the areal peak density, Digital Instruments software determines the RMS peak height, then discriminates continuous profiles above the threshold set point. In this work, the threshold value used throughout was 10% of the RMS peak height value. When RMS peak height values are low, peak count data may be affected by a spurious threshold due to either vibrations in the AFM tip caused by ambient sounds or electronic noise that is an artifact of the system. In all cases in this work, the in-plane and out-of-plane sensitivities were 0.1 μm and 0.1 nm, respectively. The roughness data reported indicate the mean of three 5 μm by 5 μm squares on the layer surface. There were 512 × 512 scan points within each scanned area, and the same instrument settings were used on each sample.

3. Results and discussion

Qualitatively, smaller peak heights and larger peak densities are characteristics of smoother deposits. AFM images of about 5 nm Ni deposits are shown in Figure 1

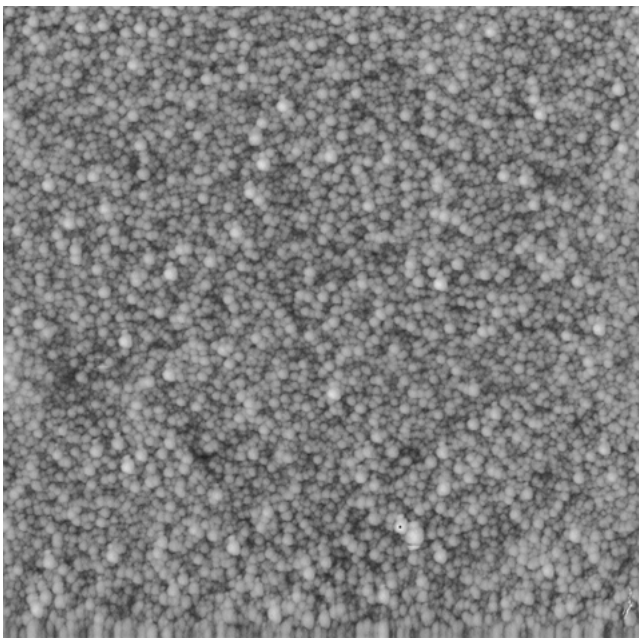

Fig. 1. AFM image of 5 nm Ni layer grown without an additive present; 5 μm by 5 μm.

(no additive used) and Figure 2 (3.25×10^{-5} M thiourea). Some differences can be discerned from these figures, but the quantitative data provide far more detail. To compare the behaviour of the different metal-additive systems in this study, and to look for trends in the data, a series of graphs was prepared.

3.1. *Ni deposition with thiourea*

Quantitative RMS peak height data for the Ni-thiourea system are shown in Figure 3. Recent work has shown

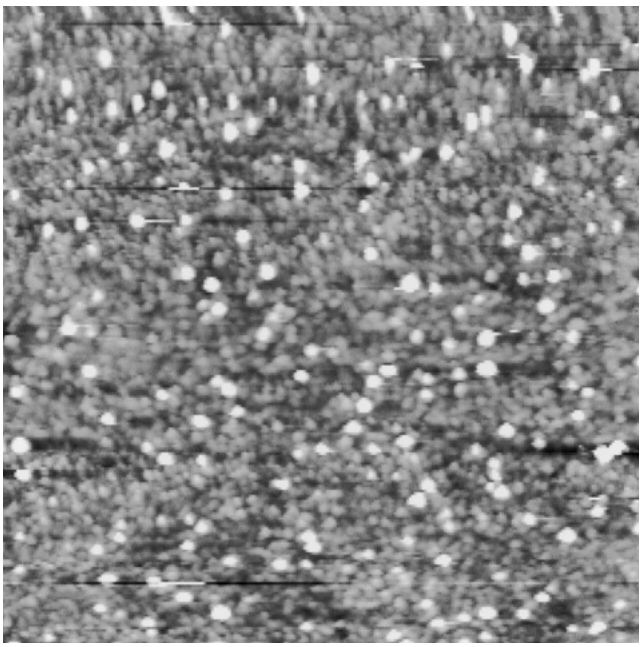

Fig. 2. AFM image of 7 nm Ni layer grown in the presence of 3.25×10^{-5} M thiourea; 5 μm by 5 μm.

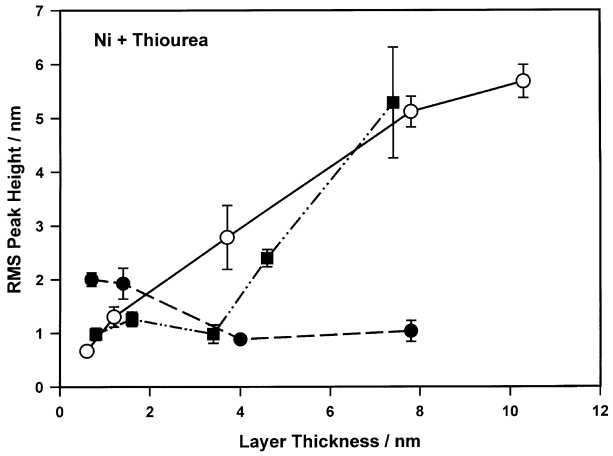

Fig. 3. RMS peak height against layer thickness for the Ni-thiourea system. Key: (○) no additive; (■) 3.25×10^{-5} M; (●) 1.22×10^{-3} M.

that the RMS peak heights of Ni layers plated from additive-free solutions increase almost linearly with film thicknesses of up to 11 nm [1]. Results for 3.25×10^{-5} M thiourea solutions indicate that Ni RMS peak heights are essentially constant at about 1 nm for layers up to 4 nm thick, then increase linearly, reaching 5.2 nm at a layer thickness of 8 nm.

When 1.22×10^{-3} M thiourea was added, RMS peak heights were increased slightly (from ~1 to 2 nm) for Ni films with nominal thicknesses up to 2 nm; for thicker films the RMS value was closer to 1 nm, significantly less than that for additive-free films. At this concentration, thiourea caused the RMS peak height to drop from 1.92 nm for a 1.4 nm nominal layer thickness to 1.03 nm at a layer thickness of 7.8 nm. This is the only system studied and the only additive concentration that had a sustained decrease in RMS roughness with increasing layer thickness.

The peak count data for the Ni-thiourea system are shown in Figure 4. The data show that peak counts for the 3.25×10^{-5} M thiourea experiments were statistically not significantly different from the additive-free runs. However, the 1.22×10^{-3} M results differed dramati-

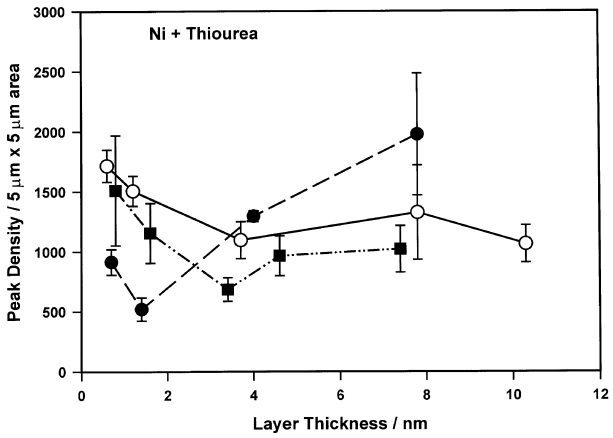

Fig. 4. Peak density against layer thickness for the Ni-thiourea system. Key: (○) no additive; (■) 3.25×10^{-5} M; (●) 1.22×10^{-3} M.

cally. With this thiourea concentration, the peak count was initially lower (~500–900 per 5 μm × 5 μm area), for layers up to approximately 3.5 nm thick; for all thicker deposits, peak densities were higher than those for the additive-free samples.

3.2. *Co deposition with thiourea*

Quantitative roughness data for the Co-thiourea system are shown in Figures 5 and 6. RMS peak heights for Co layers (Figure 5) deposited without the additive start at about 0.9 nm and increase until the layer thickness reaches approximately 6 nm, then they level off at about 7 nm. Below a layer thickness of 3.0 nm, differences in RMS height for zero, 1.25×10^{-6}, and 1.25×10^{-5} M thiourea are not statistically significantly different; for thicker layers, differences between additive-free and 1.25×10^{-6} M solutions are slight. A 39% decrease in RMS peak height for 5.0 nm layers is seen from the additive-free bath to the 1.25×10^{-5} M solution. With 1.25×10^{-3} M thiourea, the RMS peak height for a 5.0 nm deposit approximately doubled over the additive-free value. RMS height data for the Co-thiourea system indicate an optimum additive concentration around 10^{-5} M that minimizes the film's vertical roughness.

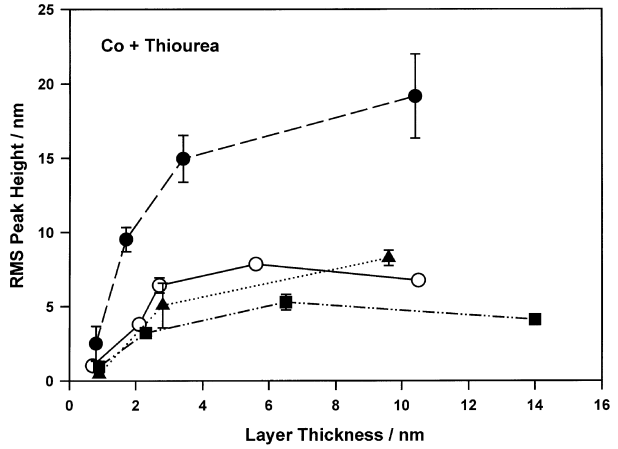

Fig. 5. RMS peak height against layer thickness for the Co-thiourea system. Key: (○) no additive; (▲) 1.25×10^{-6} M; (■) 1.25×10^{-5} M; (●) 1.25×10^{-3} M.

Co-thiourea peak count data are shown in Figure 6. The peak counts remained relatively constant at approximately 1700 per 5 μm × 5 μm area for additive-free and 1.25×10^{-6} M experiments for layers between 3 and 10 nm thick. The 1.25×10^{-6} M experiments also showed a very high initial peak count value of 5150 peaks for a 5 μm by 5 μm scanned area on a 0.9 nm layer; in part, this may reflect the low peak count threshold resulting from low RMS heights. Peak densities for the 1.25×10^{-5} M experiments seem to oscillate with increasing layer thickness. The reason for this is unknown. Runs at 1.25×10^{-3} M resulted in a very low peak count due to large but widely separated peaks and incomplete coverage of the surface. Deposited layers were estimated to cover only 10–20% of the surface and the substrate could be seen between individual peaks. In contrast to the behaviour of the Ni-thiourea system, Co nucleation appears to be suppressed by the addition of ca. 10^{-3} M thiourea.

3.3. *Ni deposition with saccharin*

Compared to Ni deposition in the absence of any organic, adding 1.25×10^{-5} M saccharin decreased the RMS peak height of a 6.5 nm layer by a factor of 4 (Figure 7). Experiments with 1.40×10^{-3} M saccharin showed an increase in RMS peak heights from those at 1.25×10^{-5} M but these were still lower than those for an additive-free solution except for the thickest layers.

Peak count results for the Ni-saccharin system fluctuated with increasing saccharin concentration (Figure 8). Compared to additive-free values a drop in peak count on a 5.0 nm layer by about 60% was observed with the addition of 6.25×10^{-6} M saccharin. If the saccharin concentration was increased to 1.25×10^{-5} M, the peak count for a 5 nm film was 80% higher than that

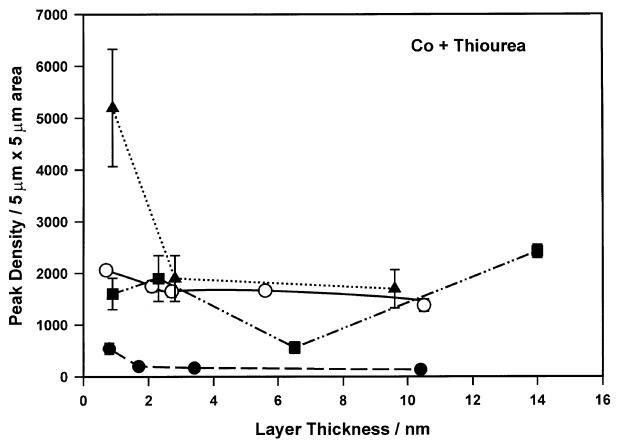

Fig. 6. Peak density against layer thickness for the Co-thiourea system. Key: (○) no additive; (▲) 1.25×10^{-6} M; (■) 1.25×10^{-5} M; (●) 1.25×10^{-3} M.

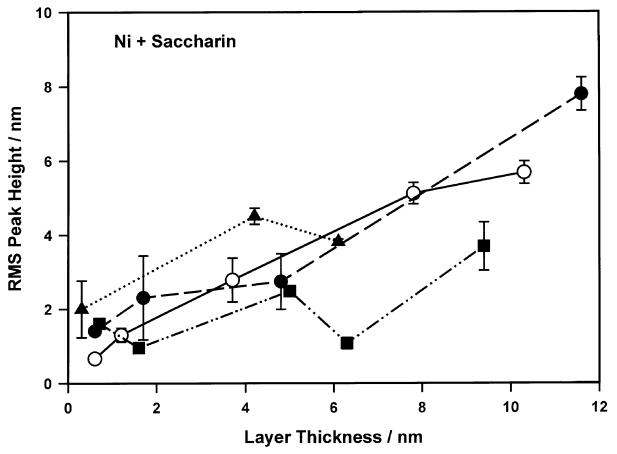

Fig. 7. RMS peak height against layer thickness for the Ni-saccharin system. Key: (○) no additive; (▲) 6.25×10^{-6} M; (■) 1.25×10^{-5} M; (●) 1.40×10^{-3} M.

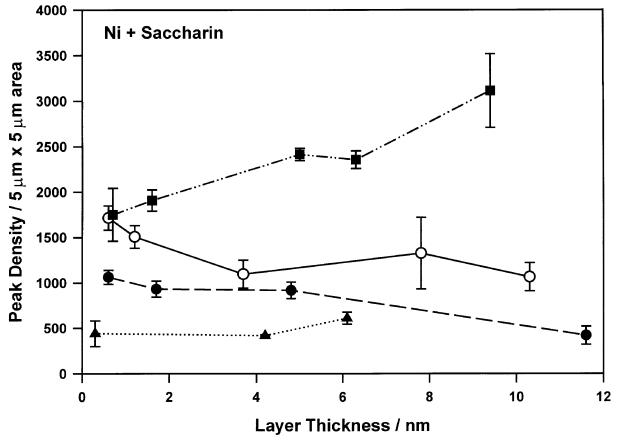

Fig. 8. Peak density against layer thickness for the Ni-saccharin system. Key: (○) no additive; (▲) 6.25×10^{-6} M; (■) 1.25×10^{-5} M; (●) 1.40×10^{-3} M.

for the additive-free case. However, a further increase to 1.40×10^{-3} M saccharin led to a peak count about 20% lower than that for 5 nm layers from an additive-free bath. This indicates an optimum additive concentration near 1.25×10^{-5} M, where the peak count is maximized.

3.4. *Co deposition with saccharin*

The last set of runs was conducted with saccharin in the Co plating bath. Saccharin was added in concentrations of 6.25×10^{-6}, 1.25×10^{-5} and 1.25×10^{-3} M. Data for the Co-saccharin system show trends similar to those from the Ni-saccharin experiments. Like the three systems discussed above, Co layers deposited in the presence of saccharin exhibited RMS peak heights that generally increased with thickness (Figure 9). Peak height results for the 6.25×10^{-6} and 1.25×10^{-5} M runs were statistically indistinguishable except for an anomalously high value at 2.6 nm in 6.25×10^{-6} M additive. Without any additive, a 6 nm Co layer had an RMS peak height of about 8 nm; this value was reduced to near 3 nm when 1.25×10^{-5} M saccharin was introduced to the bath. However, with a further increase to 1.25×10^{-3} M, the RMS peak heights increased again and were quite close to those of the additive-free experiments.

Peak count data revealed that the areal density increased with increasing saccharin concentration up to about 10^{-5} M, then decreased with $\sim 10^{-3}$ M additive (Figure 10). Results for the additive-free Co plating bath and the 6.25×10^{-6} M saccharin runs were similar, with peak counts remaining approximately constant at 1800 peaks per 5 μm by 5 μm area. Runs with 1.25×10^{-5} M saccharin had an increased peak count; the values were initially around 4800 and dropped with layer thickness to approximately 2300 peaks per 5 μm by 5 μm area at a Co thickness of 10 nm. This indicates that at a saccharin concentration of 1.25×10^{-5} M, the nucleation rate has dramatically increased from that of the additive-free bath. When the additive concentration was increased further to 1.25×10^{-3} M, the peak count remained high at 5100 peaks for a 1.2 nm layer but dropped quickly with increased layer thickness, reaching a value of 2000 for a 5 nm sample. At this point, the areal density levelled off and remained constant at approximately 2000 peaks per 5 μm $\times$ 5 μm area for deposited thicknesses up to 12 nm.

3.5. *Interpretation of RMS height–peak density crossplots*

When a sufficiently extensive set of data is available, a 2D crossplot of peak height against density provides a basis for drawing inferences about the probable growth mechanism of an ultrathin electrodeposited film. To illustrate, first consider two contrasting limiting cases (Figure 11). Assume for simplicity that nucleation is 'instantaneous' or nearly so. If the subsequent peak growth is predominantly vertical, the RMS height of nominally thicker layers increases, but the peak density should remain essentially unchanged; with RMS peak height chosen as the x-axis, the crossplot has a hori-

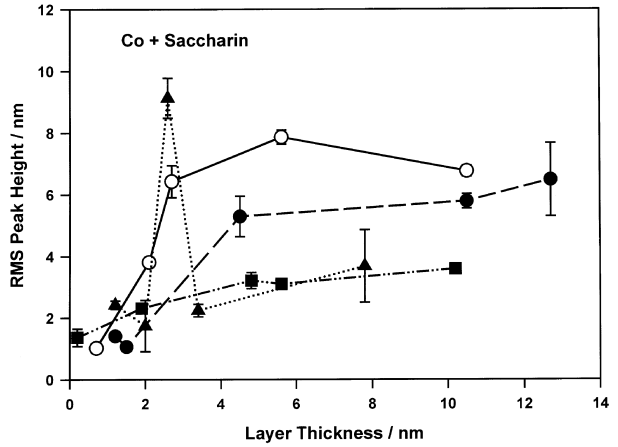

Fig. 9. RMS peak height against layer thickness for the Co-saccharin system. Key: (○) no additive; (▲) 6.25×10^{-6} M; (■) 1.25×10^{-5} M; (●) 1.25×10^{-3} M.

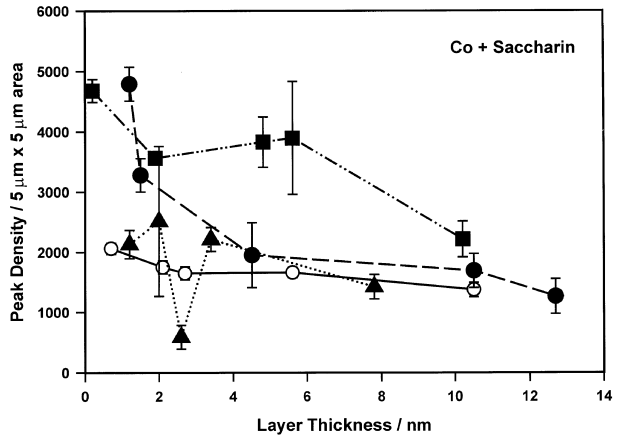

Fig. 10. Peak density against layer thickness for the Co-saccharin system. Key: (○) no additive; (▲) 6.25×10^{-6} M; (■) 1.25×10^{-5} M; (●) 1.25×10^{-3} M.

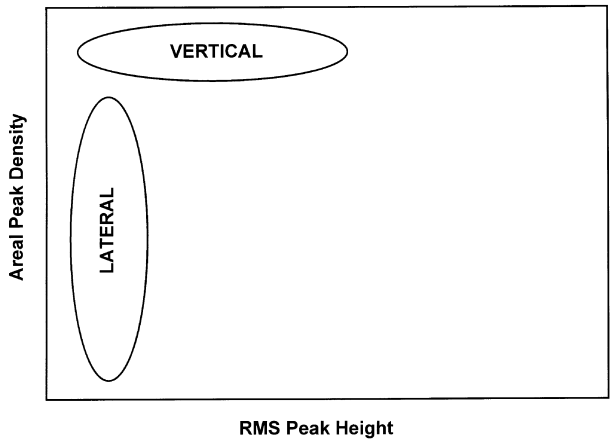

Fig. 11. Expected effect of predominant growth direction on clustering in crossplots.

zontal band of clustered points. In contrast, if peaks mainly grow laterally, the peak density decreases as adjacent peaks overlap; with little change in the peak height, a vertical band will appear in the crossplot. Intermediate cases with significant peak growth in both directions would give a band directed at an angle. If nucleation is 'progressive' but a single growth mode (vertical, lateral, or mixed vertical + lateral) predominates throughout the deposition, the same basic types of 2D crossplots would be expected. However, in these cases, a third axis, time or nominal layer thickness, can be envisioned, and the plotted points would correspond to a mixed-age population of growth peaks and would be projected onto the density against height plane. More disordered growth, as in a multinuclear, multilayer mechanism, should produce a scattered cluster of points lacking any preferred direction.

Characteristic patterns of clustered points can be seen in crossplots of the data for the four systems investigated (Figures 12–15). To facilitate comparison of the four systems, the axes are scaled in the same way for each.

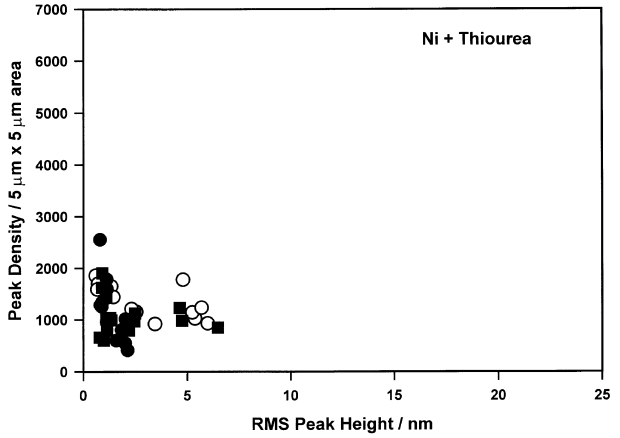

Fig. 12. Peak density against RMS peak height for the Ni-thiourea system. Key: (○) no additive; (■) 3.25×10^{-5} M; (●) 1.22×10^{-3} M.

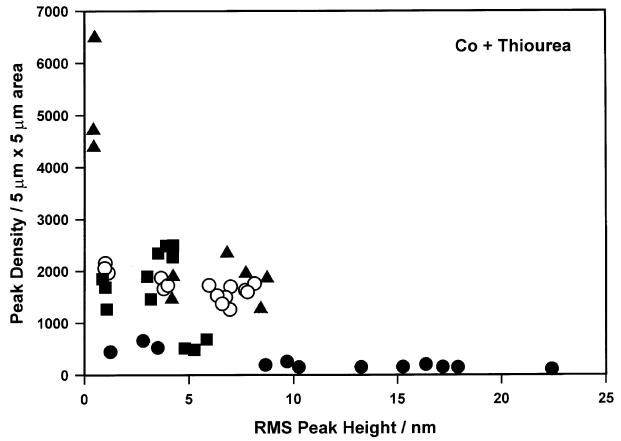

Fig. 13. Peak density against RMS peak height for the Co-thiourea system. Key: (○) no additive; (▲) 1.25×10^{-6} M; (■) 1.25×10^{-5} M; (●) 1.25×10^{-3} M.

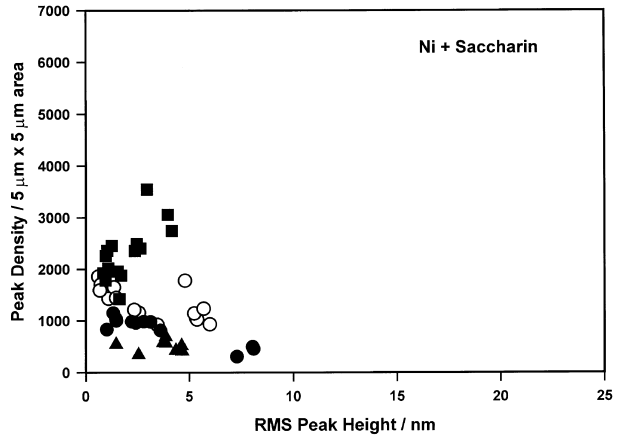

Fig. 14. Peak density against RMS peak height for the Ni-saccharin system. Key: (○) no additive; (▲) 6.25×10^{-6} M; (■) 1.25×10^{-5} M; (●) 1.40×10^{-3} M.

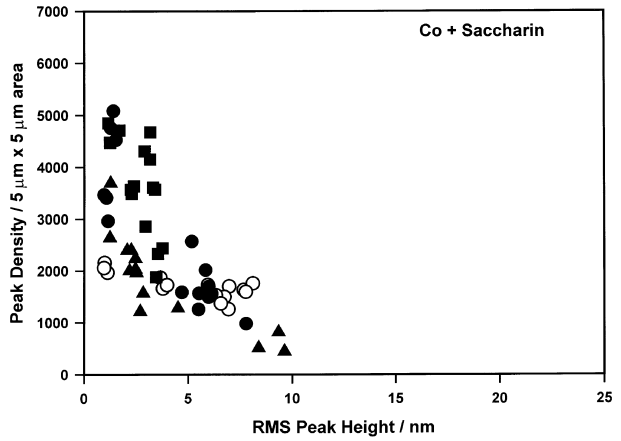

Fig. 15. Peak density against RMS peak height for the Co-saccharin system. Key: (○) no additive; (▲) 6.25×10^{-6} M; (■) 1.25×10^{-5} M; (●) 1.25×10^{-3} M.

Previous work has suggested that in additive-free nickel deposition, a multinuclear, multilayer growth mechanism

eventually becomes dominant as the layer becomes thicker [1]. The data for the Ni-thiourea system suggest a shift in the deposition mechanism with increased additive concentration. Figure 12 indicates that without thiourea, peak densities are between 1000 and 2000 for an area 5 μm on a side; with 3.25×10^{-5} M thiourea, the peak densities are more widely spread but generally lower. Peak heights are comparable in the two cases. When the thiourea concentration was increased to 1.22×10^{-3} M, peak heights were typically between 1 and 2 nm while peak densities ranged from less than 500 to more than 2500. The changes can be explained by a shift in the predominant direction of film growth from vertical with low (or zero) thiourea concentration, to lateral or mixed lateral + vertical. Figure 4 indicates that millimolar thiourea suppresses the initial nucleation and causes low initial peak counts; for deposits thicker than about 4 nm, lowered peak heights are also observed (Figure 3).

For Co deposition without additives, previous work showed that a steady-state, multinuclear, multilayer growth regime was also reached [1]. The differences in growth mode when thiourea is added in varying concentration are particularly dramatic (Figure 13). For the thinnest layers, the presence of 1.25×10^{-6} M thiourea is associated with very high peak densities and considerable scatter in the data; for somewhat thicker layers, the growth pattern is similar to that of the additive-free system. In contrast, very high peak heights and low peak counts were observed for 1.25×10^{-3} M thiourea, consistent with predominantly vertical growth with relatively little overlap of adjacent peaks. At this concentration, the initial peak count is low (Figure 6), consistent with suppression of nucleation.

Effects of saccharin on Ni deposition are strongly dependent on the concentration of the additive. The intermediate concentration of 1.25×10^{-5} M results in peak densities that are higher and span a wider range (less than 1500 to over 3500) than those seen for either 6.25×10^{-6} M or 1.40×10^{-3} M additive (Figure 14). Growth appears to be quite disordered with 1.25×10^{-5} M saccharin, as evidenced both by the correlation of increased peak density with increased RMS height (Figure 14) and by the increased peak density of the thicker layers (Figure 8). Such an increase in the peak count for thicker layers implies that nucleation is progressive and probably accompanied by multilayer growth. For both the lowest and the highest concentrations used in this study, more regular and predominantly vertical growth is suggested by the horizontal banding at low peak densities in Figure 14. Thus, for the Ni + saccharin system, the growth mechanism appears to shift twice as the additive concentration increases from micromolar to millimolar levels.

Deposition of Co in the presence of 6.25×10^{-6} M saccharin appears to lead to mixed vertical + lateral growth; RMS heights increase as the peak count decreases (Figure 15). With an increase in the additive concentration to 1.25×10^{-5} M, all measured peak heights were less than 5 nm, but peak densities ranged from under 2000 to close to 5000 (per 5 μm $\times$ 5 μm square); this pattern is characteristic of predominantly lateral growth. A further increase to 1.25×10^{-3} M saccharin leads to broadening of the peak heights, suggesting a less ordered growth mode.

4. Conclusions

Contact mode atomic force microscopy has been used to measure RMS peak heights and areal peak densities for ultrathin Ni and Co layers electrodeposited in the presence of μM to mM saccharin or thiourea. For both metals, layer roughness depends on the additive used, its concentration, and the thickness of the layer. Additive concentrations that minimize peak height and maximize peak density were identified in some cases. Crossplots of RMS height against areal density were used to identify situations in which peak height and density are correlated, and it is argued that such correlations can be characteristic of the predominant growth mechanism of an ultrathin metallic electrodeposit.

Acknowledgements

The AFM characterization was partially supported by National Science Foundation grants DMR-9205197 and CHE-9709273; the assistance of Kerry Hipps is gratefully acknowledged. John Yates helped with preparation of the substrate.

References

1. R.F. Renner and K.C. Liddell, *J. Mater. Res.* **15** (2000) 458.
2. J. Edwards, *Trans. IMF* **39** (1962) 33.
3. J. Edwards and M. Levett, *Trans. IMF* **41** (1964) 147.
4. J. Edwards, *Trans. IMF* **41** (1964) 140.
5. A. Bodnevas and J. Zahavi. *Plat. Surf. Finish.* Dec. (1994) 75.
6. J. Edwards, *Trans. IMF* **39** (1962) 52.
7. J. Matulis, A. Bodnevas and M. Vainilaviciene, *Plating* **56** (1969) 1147.
8. Y. Nakamura, N. Kaneko, M. Watanabe and H. Nezu, *J. Appl. Electrochem.* **24** (1994) 227.
9. C-Z. Gao, Y.L. Lu, H-T. Wang and S-B. Yue, *Trans. IMF* **77** (1999) 192.
10. J. Macheras, D. Vouros, C. Kollia and N. Spyrellis, *Trans. IMF* **74** (1996) 55.
11. V. Darrort, M. Troyon, J. Ebothe, C. Bissieux and C. Nicollin, *Thin Solid Films* **265** (1995) 52.
12. I. Tabakovic, S. Riemer, V. Inturi, P. Jallen and A. Thayer, *J. Electrochem. Soc.* **147** (2000) 219.
13. T. Osaka, T. Sawaguchi, F. Mizutani, T. Yokoshima, M. Takai and Y. Okinaka, *J. Electrochem. Soc.* **146** (1999) 3295.
14. T. Osaka, M. Takai, Y. Sogawa, T. Momma, K. Ohashi, M. Saito and K. Yamada, *J. Electrochem. Soc.* **146** (1999) 2092.
15. T. Osaka, M. Takai, K. Hayashi, Y. Sogawa, K. Ohashi, Y. Yasue, M. Saito and K. Yamada, *IEEE Trans. Magnetics* **34** (1998) 1432.
16. E. Chassaing, *J. Electrochem. Soc.* **148** (2001) C690.
17. J.J. Kelly, P.E. Bradley and D. Landolt, *J. Electrochem. Soc.* **147** (2000) 2975.
18. J.J. Kelly, P. Kern and D. Landolt, *J. Electrochem. Soc.* **147** (2000) 3725.
19. R.F. Renner, MS thesis, Washington State University (1999).